

SIMULATIONS OF ‘BOTTOM-UP’ FILL IN VIA PLATING OF SEMICONDUCTOR INTERCONNECTS

Uziel Landau¹, Eugene Malyshev², Rohan Akolkar¹, and Sergey Chivilikhin¹

**²Department of Chemical Engineering
Case Western Reserve University
Cleveland, OH 44106**

uxl@po.cwru.edu

and

**¹L-Chem, Inc
Beachwood, OH 44122**

cdw@l-chem.com

Key Words: copper plating, ‘superfill’, metallization, additives, current distribution, via plating, trench plating

©2003, Uziel Landau and L-Chem, Inc.

Prepared for Presentation at the Metallization Symposium, AIChE Annual Meeting, Nov. 17-18, 2003,

Unpublished

AIChE Shall Not Be Responsible For Statements or Opinions Contained in Papers or Printed in its
Publications

Abstract

Copper metallization of semiconductor interconnects hinges on the ability to obtain ‘bottom-up’ plating of the sub micron-scale features on the wafer surface. A special additives combination, that modifies the deposition kinetics as a function of position along the via depth is the key to the process. We present here numerical simulations of the via plating process using an electrochemical computer aided design software (“Cell-Design”). Position dependent electrode kinetics are combined with a convective-diffusion model that accounts for the external flow. The time-dependent deposit growth process is simulated. Analysis of the role of the various controlling process parameters is presented.

Introduction

The successful implementation of the process for interconnect metallization by copper electroplating, hinges on the ability to completely fill micron-scale trenches and vias with electroplated copper [1, 2]. Defect-free fill of dual damascene structures with 10:1 aspect ratios and diameters down to 0.1 μm is routinely achieved across large (200 and 300 mm) wafers, populated with hundreds of microprocessor, each incorporating in excess of 60 million transistors adding up to hundreds of millions of interconnects per wafer. All these vias and trenches must be completely filled with plated copper. To achieve this, copper may not be plated in its ‘normal’ mode where the top rims build-up first in a dog-bone fashion due to enhanced transport and a higher field at the small curvature, generating a trapped void [Fig. 1 (a)]. Nor is it acceptable to plate conformally (by suppressing the deposition process through the use of excess additives) as shown schematically in Fig.1 (b). The only acceptable process is that depicted in Fig. 1 (c), where the copper growth starts at the bottom of the via and rapidly progresses upwards. Since not only the bottom but also the top and sidewalls of the via are metallized by copper seed, and since the plating of the via emanates from its top (highest transport and field), it is difficult to achieve this ‘bottom-up’ fill.

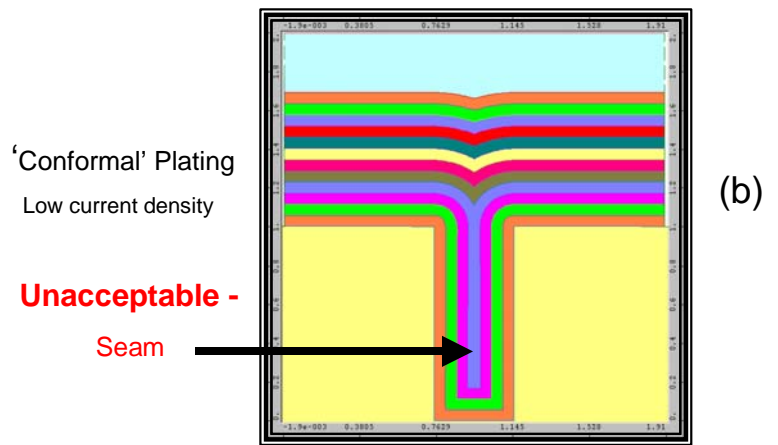
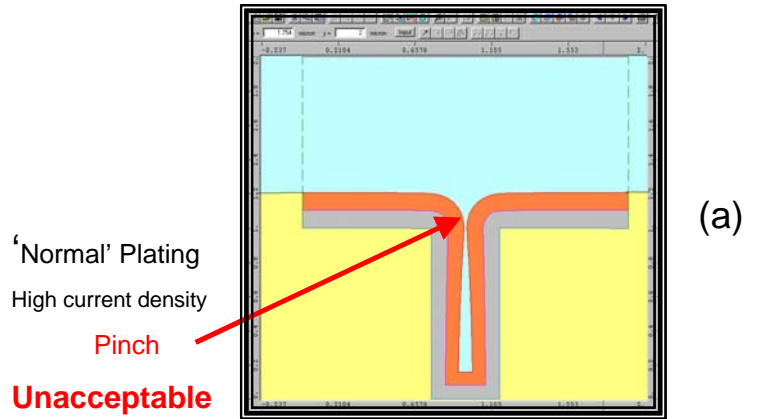
The key to the implementation of the process has been IBM’s discovery [1, 2] that the bottom-up fill can be achieved through the use of a special mix of plating additives that by differential adsorption on the flat surface and within the via can affect the ‘bottom-up’ fill. The additives mix typically contains a relatively large, slow diffusing, suppressing additive (e.g. polyethylene glycol) that preferentially adsorbs on the flat surface and the rim of the vias and slows down the deposition at those locations, in combination with another additive (e.g. an organic sulfur compound) that preferentially adsorbs within the via and enhances deposition (or negates the effects of the suppressing additive) at its bottom.

Scaling Issues

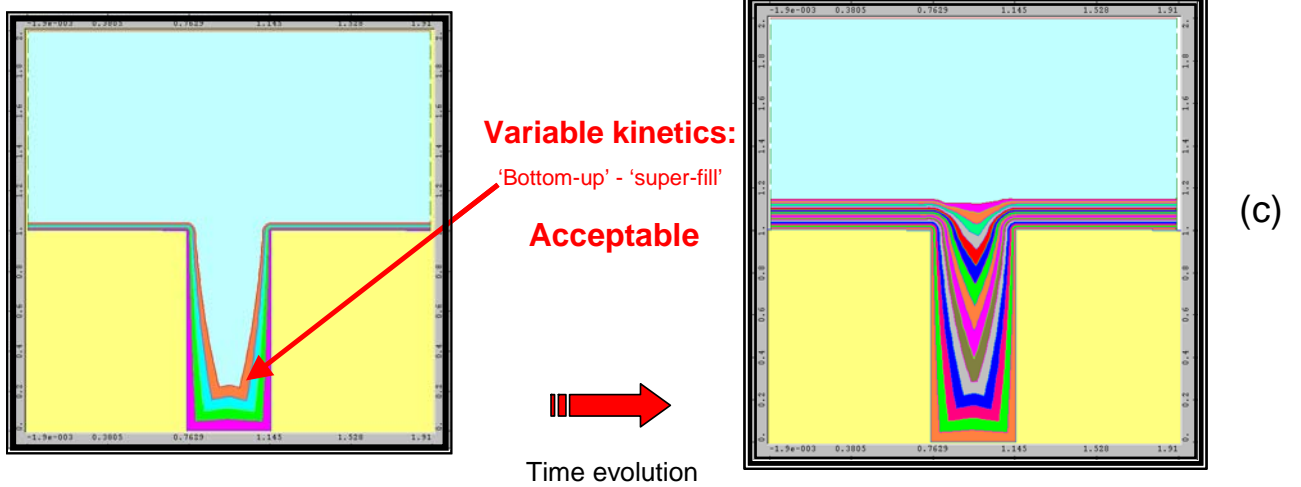
Since the microscopic and macroscopic current distributions on the wafer are carried on such widely different scales (μ vs. cm), they are controlled by different mechanisms and must be analyzed separately. This difference in scales, which leads to different controlling mechanisms, is the key to the successful accomplishment of the process, since the design objectives on the two scales are quite different. On the microscale a highly non-uniform current distribution which leads to the bottom-up fill is sought, while on the wafer scale, a highly uniform distribution is important. The distribution on the wafer scale is controlled primarily by the plating cell configuration, the conductivities of the electrolyte and the substrate, the current density, and to a lesser extent, by the electrolyte flow. The distribution on the feature scale, on the other hand, is dominated by kinetics and diffusion.

Fig. 1: Different modes of gap-fill. Cross-sections showing time-stepping through simulated plating of a $0.4\ \mu$ wide x $1\ \mu$ deep trench. **(a) Top:** 'normal' plating with preferential coverage at the rim. **(b) Center:** Conformal plating, tracing the substrate profile. **(c) Bottom:** 'Superfill' With plating initiated at the bottom.

Simulations were done using "Cell-Design" software [3].



Deposit Growth Profiles



Wafer-Scale (Macroscopic) Current Distribution

The current density and the deposit thickness distribution on the wafer scale is characterized, not considering the substrate seed resistance, in terms of the Wagner number, as discussed elsewhere in this Symposium [4]. The Wa number represents the ratio of the activation resistance (R_a), of the electrode reaction, which typically enhances uniformity, to the ohmic resistance of the electrolyte (R_Ω). The latter is geometry dependent and usually causes non-uniformities.

$$Wa = \frac{R_a}{R_\Omega} = \frac{\kappa}{l} \left(\frac{\partial \eta_a}{\partial i} \right) \sim \frac{\kappa b}{li} \quad [1]$$

Here, κ is the electrolyte conductivity; l is the characteristic length (wafer scale) and $\partial \eta_a / \partial i$ is the slope of the polarization curve. The latter is controlled by the additives composition. The approximation on the right of Eq. 3 pertains to the ‘Tafel regime’ where most copper deposition takes place. Here, b is the ‘Tafel slope’ ($= RT/\alpha F$). For uniform distribution, a high Wagner number is desired, corresponding to high electrolyte conductivity, low current density, and a high slope of the polarization curve. Appropriate cell design, including the application of current shields, can, however, compensate for current density non-uniformities even when the Wa number is low.

The Microscopic (Feature-Scale) Current Distribution

The characteristic distance on the feature scale is of the order of a micron, many orders of magnitude smaller than that of the wafer. As a consequence, the controlling mechanism for the current distribution shifts from the potential field to mass transport control [5]. The length scale at which mass transport limitations become more significant than the ohmic resistance is given [5] by:

$$l_{crit} < \frac{\kappa RT}{nF i_L \left(1 - \frac{i}{i_L}\right)} \quad (\text{for mass transport to be controlling}) \quad [2]$$

Applying conditions typical to copper plating, we find that the critical length below which mass transfer becomes dominant is of the order of a few hundred microns. Accordingly, the current distribution within the micron-scale features is influenced primarily by mass transport with negligible electric field effect. It should be emphasized that this scaling analysis compares only the relative importance of mass transport to electric migration. Kinetics resistance, which is not scale-dependent, will typically be the overall dominant resistance in small scales, prevailing over both the mass transport and the ohmic resistances. It is actually this kinetics resistance that is being manipulated through different position-dependent adsorption of the additives to give the ‘super-fill’.

Based on this analysis, it is not meaningful to characterize the microscopic current distribution in terms of the Wa number, since the latter is based on the ohmic resistance, whereas on the micro-scale, the concentration field is more important. Instead, the micro-leveling parameter, L , has been formulated [5], replacing (as the source for non-uniform flux) the ohmic resistance by mass transfer resistance and comparing it to the kinetics resistance:

$$L = \frac{R_a^*}{R_c^*} = \frac{\left| \frac{\partial \eta_a}{\partial i} \right|}{\left| \frac{\partial \eta_c}{\partial i} \right|} = \frac{n i_L \left(1 - \frac{i}{i_L}\right)}{\alpha i} \quad [3]$$

A large value of L ($L \gg 1$) implies kinetics resistance dominance. Typically, this corresponds to a uniform current distribution on the micro-scale, since the kinetics is usually not geometry dependent. If, however, additives adsorption, which controls the deposition kinetics, is not uniform, as the case with bottom-up fill is, a high value of L does not warrant uniformity. It implies, however, that the additives distribution will dominate the current distribution, as practiced in the bottom-up fill.

Flow Effects

The plated wafer is typically subject to flow due to the wafer rotation ($\sim 40 - 80$ RPM) and to impinging (fountain) flow ($\sim 2-8$ gpm). As has been analyzed elsewhere in this Symposium [4], under typical operating conditions, most of the convective flow is due to the rotation. A typical flow field in wafer plating applications has been simulated using 'Cell-Design' software [3] and is displayed in Fig. 2.

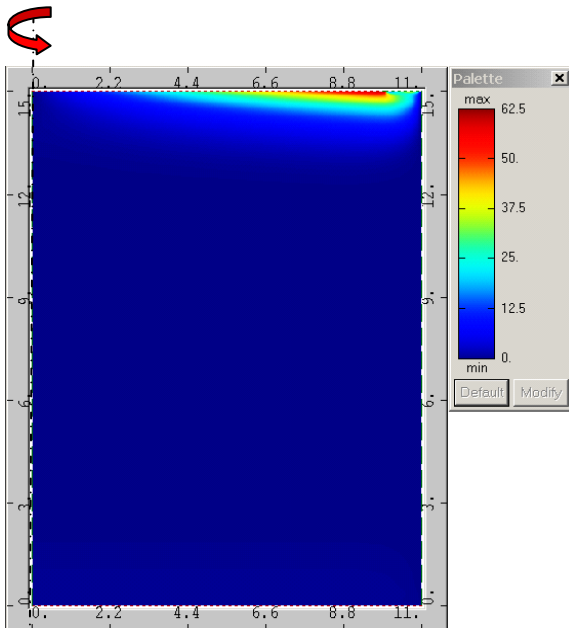
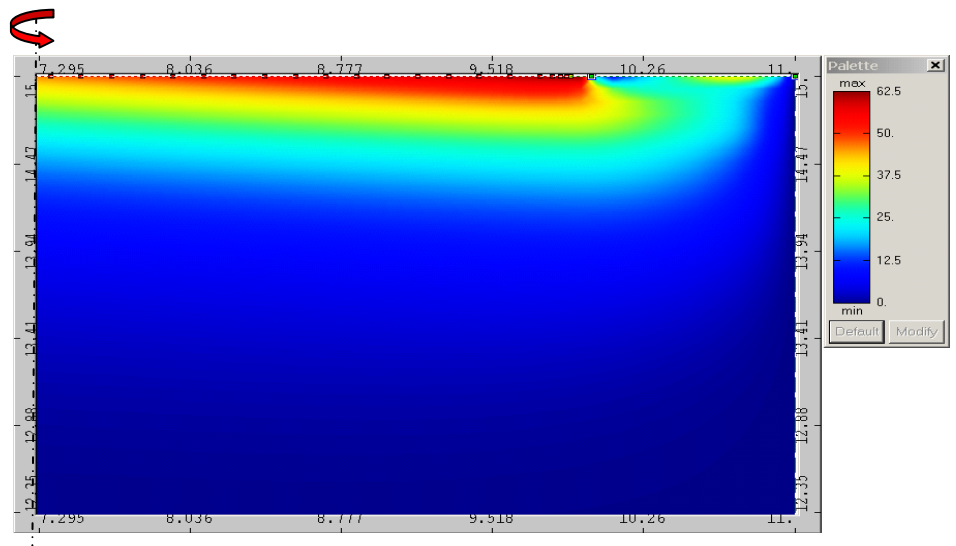
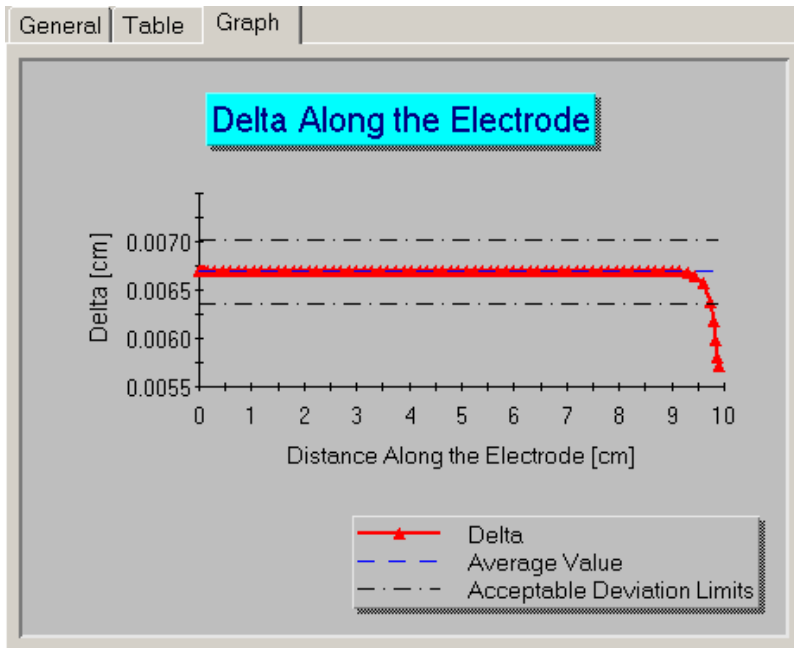


Fig. 2: Flow field in a typical wafer plating application. The 200 mm diameter wafer is rotated at 60 RPM. It is also subject to 4 GPM uniformly distributed impinging flow. A 1 cm side gap is provided between the wafer rim and the cell sidewall for electrolyte egress. As noted, little velocity exists in the cell and most of the velocity gradients occur next to the wafer. (Simulated by 'Cell-Design' software).

Fig. 3: Magnified (zoomed in) view of the flow-field shown in Fig 2.



Although the velocity field shown in Figs. 2 and 3 appears non-uniform across the wafer, the (mass transport) boundary layer thickness as computed by 'Cell-Design' and displayed in Fig. 4 (below) indicates that over most of the wafer mass transport is quite uniform, with variations occurring only within the last 8 mm of the radial distance, closest to the edge.



Fig, 4: The boundary layer thickness (mass transport) along the wafer as computed by 'Cell-Design'. Flow conditions are identical to those in Figs. 2 and 3. Note that the boundary layer thickness is constant over the majority of the wafer, deviating only in the last 8 mm closest to the rim.

On the flat regions of the wafer, the copper is typically plated far below its limiting current, and flow effects on the copper mass transport are expected to be small. This is important to note, because although the boundary layer thickness across the entire wafer is about uniform, as shown in Fig. 4, minor variations may still exist. Since additives are present in minute amounts, those additives that are consumed by the electrode reactions, or adsorbing additives during the transition time, until a steady-state additives concentration on the surface is established, are expected to be more sensitive than the copper to flow variations. The effect of flow on the deposition kinetics is analyzed in the following section (polarization data).

One may assume that the macroscopic flow will lead to a convective flow pattern within the vias, phenomenon that is commonly encountered in larger features. Computational analysis, as shown in Figs. 5 and 6, indicates, however, that the secondary flow field within the vias and trenches is negligible. This is due to their very small size.

The fact that convective flow effects within the vias are negligible is important, because, if such effects were present, we would expect to note their influence on the plating process. Since the vias are distributed across the wafer and are subject to different tangential and radial velocities, such effects could depend on the via position and therefore be highly non-desirable. We conclude that we may

analyze the transport within the vias as if it was dominated by stagnant diffusion, subject to the boundary layer imposed by the macroscopic flow field.

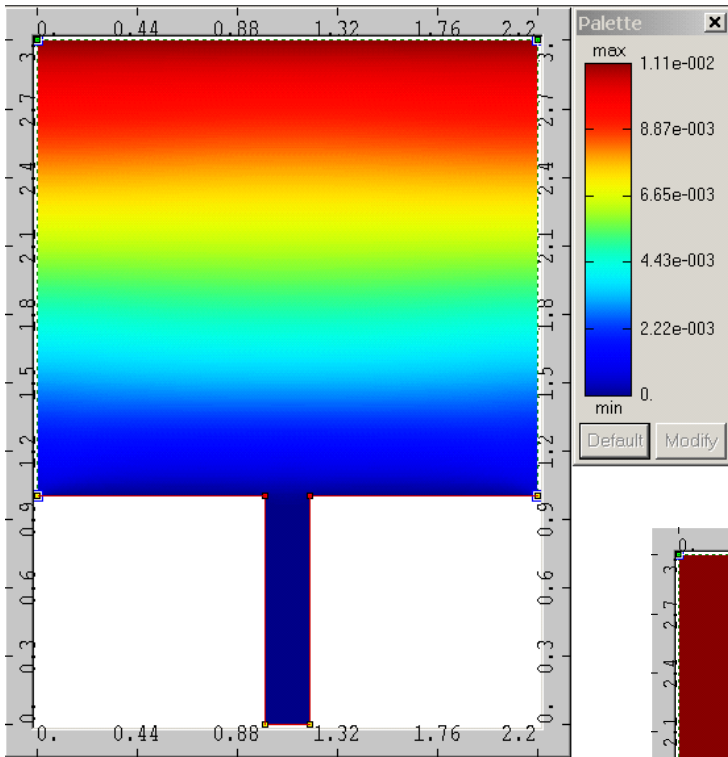


Fig. 5: Flow field near and within a 0.2 μ wide x 1 μ deep trench subject to the macroscopic flow displayed in Figs. 2 and 3. As noted, no secondary flow is noted within the trench.

Computed by 'Cell-Design'.

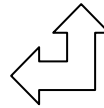
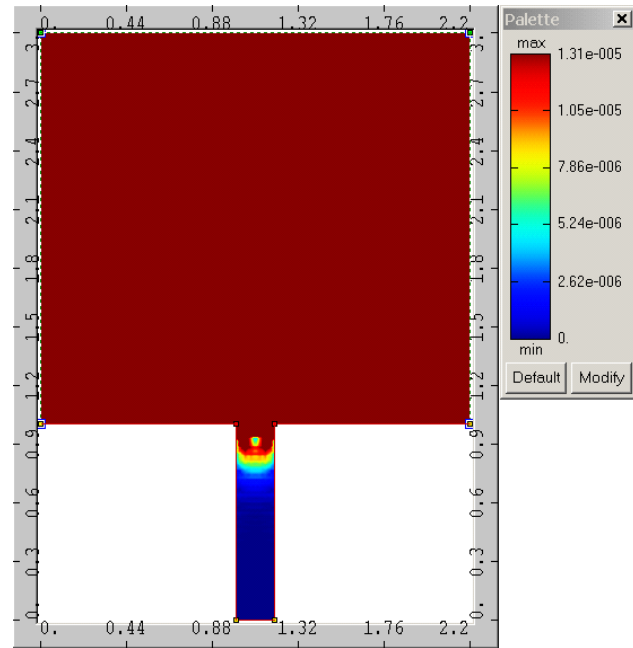
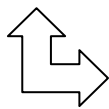


Fig. 6: A highly magnified flow 'palette' for the flow field shown in Fig. 5, indicating the presence of an extremely weak (by about 3-4 orders of magnitude) circulation 'eddy' at the mouth of the via.



Deposition Kinetics and Additives Adsorption:

The deposition process, particularly on the micro-scale, critically depends on the deposition kinetics. The bottom-up fill hinges on the complex interaction between various classes of the plating additives that are commonly used [6,7]: (i) chloride ions (~ 40 to 100 ppm), which adsorbs particularly at grain boundaries and appears to enhance the activity of the other additives; (ii) polyether e.g., polyethylene glycol –'PEG' at ~ 100 – 200 ppm, which acts as an inhibitor to the copper deposition; (iii) an organic disulfide, e.g., Bis(3-sulfopropyl)-disodium-sulfonate or 'SPS', at about 20 - 80 ppm, which serves as an accelerator; and sometimes also (iv) a quaternary nitrogen compounds in the few ppm range, which

serves mostly to slow down the accelerated deposition within via clusters, once the deposit reaches the level surface. Despite the fact that the exact mechanism by which the different additives classes affects the deposition process is not clear, it has been found empirically that the first three of the additives groups (chloride, polyether, and the di-sulfide) are essential for the bottom-up gap fill process and no commercial process, to our knowledge, operates without some such combination, despite considerable technological and economic motivation to reduce the complexity of the chemical system.

Although the detailed mechanism by which the additives affect the deposition process remains controversial, numerous observations and experiments [e.g., 7,8] provide insight into their role: (a) The bottom-up fill *progresses rapidly*, with 1 μ deep vias filling in less than 1 min. This corresponds to a local current density within the via of about 60 mA/cm², while the average current density on the wafer is typically of the order of 10 mA/cm², indicating strong inhibition on the top surface, and acceleration of the plating on the via bottom. (b) Experiments [7,8] indicate that *transient effects* during the first minute or so of plating are critical, particularly since the via fill is completed during this time period. The deposition kinetics observed shortly after the substrate exposure to the electrolyte are quite different than at steady-state, which may take many minutes to establish [7,8]. Industrial practice indicates that it is important to initiate plating shortly after wafer immersion in the electrolyte. Some controversy surrounds, however, this practice, with claims that the nearly instantaneous plating initiation is driven by the need to minimize seed dissolution. This practice is maintained, however, also in non-acidic and de-aerated electrolytes that should not accommodate seed dissolution. (c) Significant *interactions* occur between the additives groups, and the bottom-up fill cannot be simulated by simple superposition of the activity of the single additives. For example, the SPS by itself is only a very moderate accelerator for copper deposition, however, in combination with PEG it negates much of the strong inhibition produced by the PEG [7,8]. (d) Fluid-flow computations, such as shown above, and experimental evidence indicate that convective flow within the vias is minimal, and transport proceeds mostly by diffusion through a substantially stagnant electrolyte within the via. (e) PEG is not consumed in the plating process and its concentration remains essentially intact, even after plating thousands of wafers from a relatively small volume electrolyte. This indicates that no net transport of the PEG towards the surface is expected during steady-state, and except for an initial period of its build-up on the surface, no steady-state PEG concentration gradient is expected [7,8]. This is in contrast to some models that assume PEG steady-state flux and concentration gradients. (f) SPS is consumed by the plating process, with at least portion of the sulfur being incorporated within the deposit. (g) The PEG adsorption kinetics are fast, and therefore PEG is expected to be transport limited [7,8]. (h) SPS adsorption kinetics are slow and therefore it is expected to be kinetically limited [7,8].

A number of bottom-up simulations have been proposed in the literature [e.g., 10-15]. Initial publications by IBM scientists [10,11] modeled the additives transport towards the via surface assuming either zero surface concentration (limiting current) or a constant surface flux, in combination with Langmuir-type adsorption isotherms. The effect on the deposition kinetics was through a blocking mechanism. Although bottom-up fill was simulated using this approach, the models involve a number of arbitrary adjustable parameters and assume steady-state additives diffusion towards the electrode.

West et al [12] present a steady-state via fill model where the additives are assumed to be diffusion controlled. Adsorption isotherms provide the surface coverage. The variable accessibility to transport of the via sidewalls leads to a varying additives concentration, resulting in different deposition rates. No additives interactions or transient effects are considered. Josell *et. al.* [13] proposed a curvature

enhanced coverage mechanism where the ‘bottom-up’ fill occurs due to catalytic surface species (sulfides) concentrating at the bottom of the trenches.

Georgiadou *et al* [14] presented a quasi-steady-state numerical model for Cu electrodeposition in trenches accounting for convective flow, additive transport, and the shape change profile during deposition. This model has been recently extended [15] to account for unsteady-state diffusion under pulse and periodic reverse plating. The models simulated ‘super-fill’ behavior, however, the authors did not provide a detailed comparison with experimental fill data, nor did they consider multi-additives systems.

A plausible bottom-up fill mechanism, supported by experimental evidence, has been recently suggested by Akolkar and Landau [7,8]. The model first recognizes that as the wafer is initially immersed, the vias are instantaneously filled by the electrolyte through capillary action, carrying with it the bulk additives concentration. The PEG present within the via adsorbs nearly instantaneously on the sidewalls and bottom, however, this initial amount corresponds to a negligible surface coverage. Additional PEG must diffuse from outside the via, however, this process is relatively slow, due to the moderate diffusion coefficient of PEG. During this time ‘delay’, the SPS, which is not transport limited due to its higher diffusion coefficient, adsorbs on the bottom regions within the via, bringing about accelerated growth, and just as importantly, protecting these regions in the short-term from further coverage by inhibiting PEG. The ratio of electrolyte volume to surface is much higher on the top surface of the wafer, which gets rapidly covered by PEG and is therefore inhibited. A more detailed discussion of the mechanism is available in Refs. [7,8,9].

Rather than employing here a complex additives model, that requires invoking mechanistic assumptions, we use, instead, a more robust approach of simulating the bottom-up fill. We apply, in a time-stepped moving boundaries computational deposition model (implemented in ‘Cell-Design’ software), global kinetics parameters that can be directly measured. For the top surface, we import polarization data measured on a rotating disk electrode in an additives mix typical to that employed in copper metallization. The kinetics in this region undergoes a transition during the first few minutes of deposition. Initially, rapid PEG adsorption dominates, causing high passivation. As time proceeds, slower SPS adsorption takes over, negating the PEG passivation. This transition can be directly measured [7,8]. The bottom region within the via is under a different additives regime. Because of the high surface area to volume ratio within the via, there is insufficient amount of additives within the via electrolyte to provide significant surface coverage [8,9]. Essentially all adsorbed additives must be provided through diffusion. PEG replenishment, is diffusion limited. Akolkar and Landau have shown [9], that the time constant for the sidewalls coverage by the diffusing PEG is highly non-linear, resulting in rapid PEG coverage of most of the sidewalls, but not of the bottom region. Consequently, the sidewalls, except for a narrow region (~10%) at the very bottom, will be rapidly covered by PEG and therefore will exhibit polarization similar to that of the top surface. Because of the non-linear coverage vs. penetration depth, the bottom, on the other hand, takes a long time to be covered by PEG. This time delay, allows the slower reacting but faster diffusing SPS to adsorb at the bottom of the via, enhancing the deposition kinetics at this region. Experiments show, that once a region is covered by the accelerating SPS, the inhibiting PEG can no longer displace it appreciably [7,8].

Although this ‘macroscopic’ approach will not elucidate the detailed additives interaction, it relates the process parameters, including the current density and the via geometry, to the gap-fill characteristics. Moreover, it employs only clearly measurable polarization parameters and does not incorporate any adjustable parameters or a controversial mechanism.

Typical polarization data, used in the modeling is shown in Fig. 7 (linear presentation) and Fig. 8 (semi-logarithmic or 'Tafel' presentation).

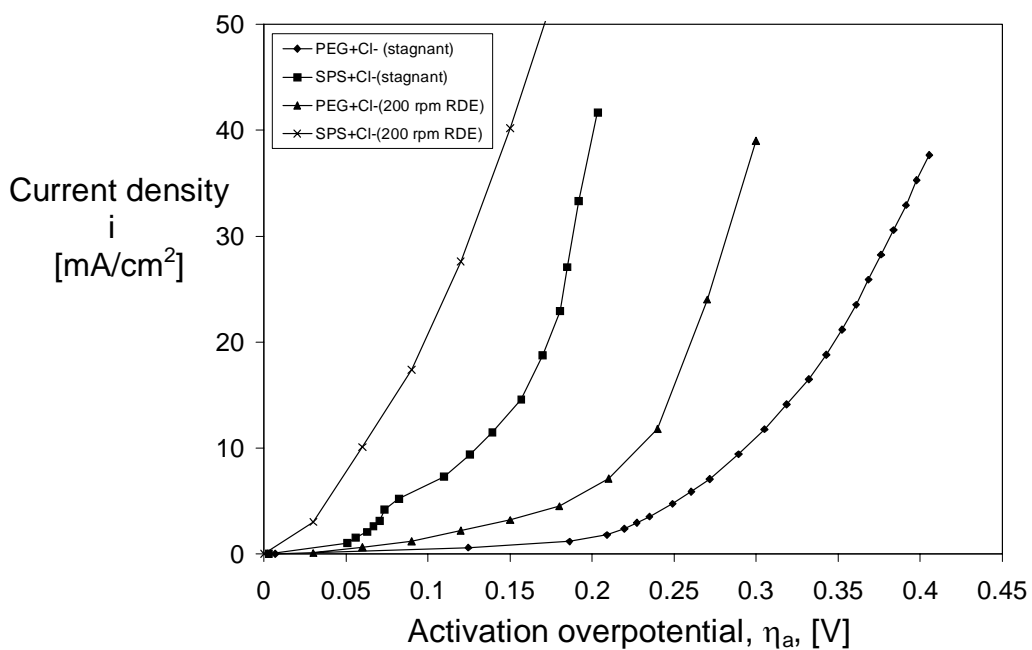


Fig. 7: Polarization data for additives mixtures measured on a rotating disk

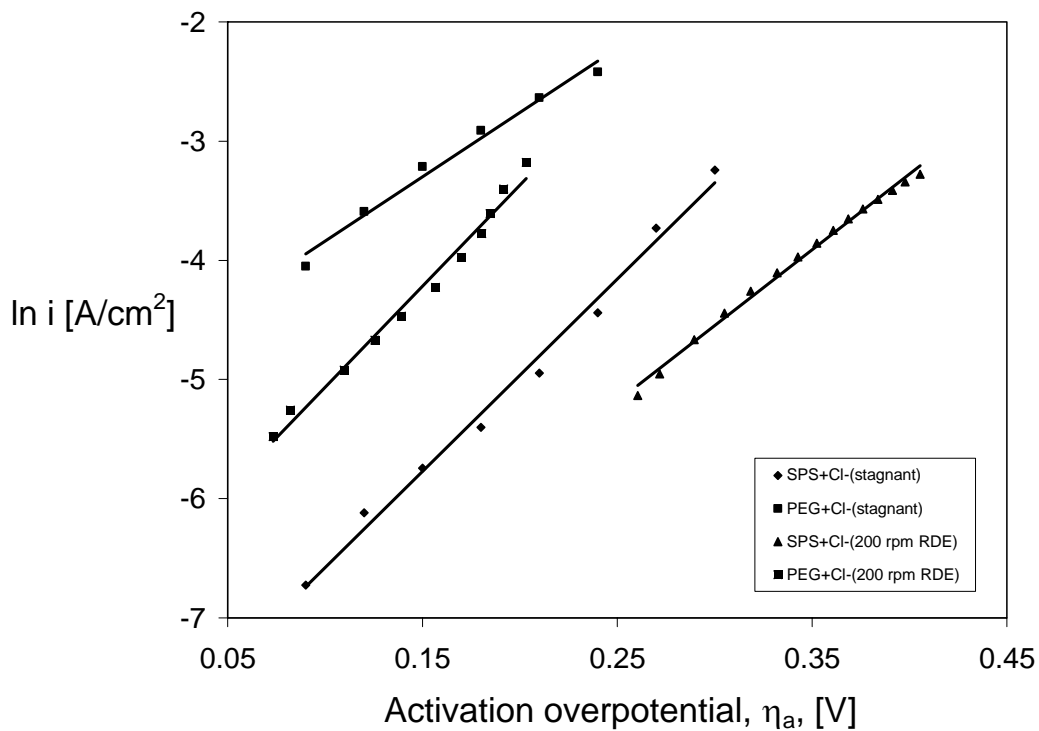


Fig. 8: The polarization data of Fig. 7 represented as a semi-logarithmic or 'Tafel' plot.

Via Fill Simulations

Simulating the via/trench fill requires solving the Nernst-Plank equation for ionic transport:

$$\frac{\partial C_j}{\partial t} = \nabla(D_j \nabla C_j) + z_j F \nabla(u_j C_j \nabla \Phi) + v \nabla C_j \quad [4]$$

The unknowns are all the species present C_j , and the electric field, ϕ . The equation also requires knowledge of the local fluid velocity (\mathbf{v}), which necessitates a simultaneous numerical solution of the flow field. However, as discussed above, the region close to the via, is substantially stagnant, and the only fluid-mechanical information required is the thickness of the equivalent Nerst type diffusion layer. This information is readily extracted from computational fluid mechanics software, such as those shown above by Cell-Design. For a typical wafer rotating at 60 RPM with an impinging flow of 4 GPM, the equivalent mass transport boundary layer is about 65 μ . Also, as has been discussed above, at short length scales, such as in the modeling the filling of a single via or a trench, the ohmic resistance is negligible in comparison to the diffusion resistance. Since we are interested only in transport of copper, and the effects of variations in the sulfate or proton concentrations affect mainly the conductivity, which has only a marginal role here, we can reduce the set of equations [4], to a single Eqn. for the copper ion. Lastly, all unsteady-state effects will be represented by time stepping a pseudo-steady-state equation. Consequently Eqn. [4] is reduced to the much simpler Laplace's Eqn. for the copper ion concentration:

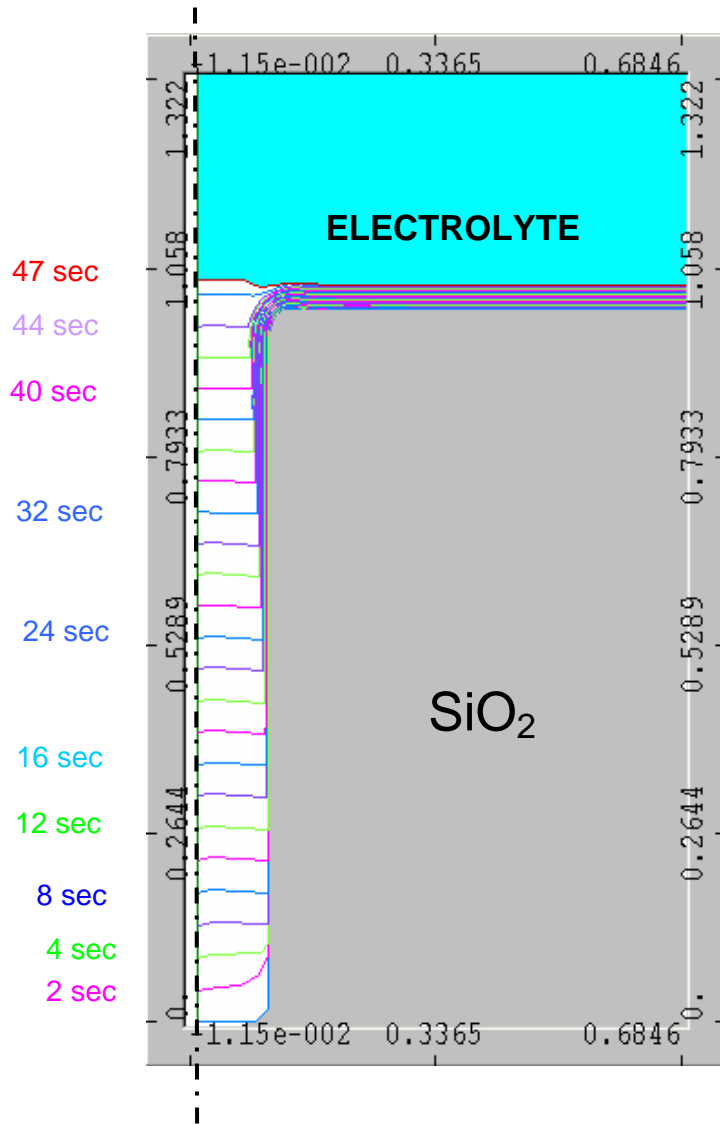
$$\nabla^2 C = 0 \quad [5]$$

The electrode kinetics control the electrode boundary conditions. The latter are affected by the copper concentration near the electrode. In the presence of plating additives, the kinetics are also significantly affected by the concentration of the additives at the electrode, their flux, their adsorption kinetics, and their interactions. These are quite complex, and their mechanism is still controversial, as shown by Akolkar and Landau in a different presentation at this symposium [8], are time-dependent. As stated above, rather than attempting controversial mechanistic models, we import into Cell-Design kinetic parameters that have been measured on a rotating disk electrode for a solution based on 70 ppm Cl^- + 200 ppm PEG + 50 ppm SPS. For the top surface and the sidewalls we implement kinetics that are at short time dominated by rapid PEG adsorption with an exchange current density, $i_0 = 3.1 \mu\text{A}/\text{cm}^2$, and $\alpha_c = 0.9$. These kinetics become gradually depolarized (most likely by the adsorption controlled SPS displacing the PEG), with $i_0 \sim 50 \mu\text{A}/\text{cm}^2$ after one minute. Eventually (after a few minutes) the kinetics correspond to the steady-state values presented in Figs. 7 and 8. Since we are time-stepping the numerical solution, we assign the proper kinetics to the simulation time-step. At the bottom of the via, we assign, as discussed in the previous section, kinetics measured in the absence of PEG, with only SPS+ Cl^- present. The corresponding kinetics parameters are $i_0 = 1.22 \text{ mA}/\text{cm}^2$, and $\alpha_c = 0.83$. Any PEG arriving later to this fast propagating surface, cannot easily replace the strongly bound SPS.

The simulation is time-stepped through the entire deposition period. We make use of Cell-Design's moving boundaries capability, which recalculates the deposit profile after each time step and sets it as the new electrode boundary for the subsequent time step. Sample via fill simulations are shown in Figs. 9 and 10. The kinetics of Fig. 9 are based on the data presented. In Fig. 10 we have assumed a faster (double) relaxation of the inhibited kinetics on the top surface and the sidewalls, with $i_0 = 92 \mu\text{A}/\text{cm}^2$ after 50 sec. This corresponds to a current density of $6.8 \text{ mA}/\text{cm}^2$ on the top surface.

Fig. 9: Deposit growth simulation by time stepping, using the moving boundaries feature of 'Cell-Design'. Except for the last 1 sec step, all steps were 2 sec.

Under the simulated conditions the hole filled after about 47 sec. The current density was adjusted to about 60 mA/cm² within the via ($i_0 = 1.22 \text{ mA/cm}^2$, $\alpha_c = 0.83$) by setting the overpotential to -0.124V. This corresponded to an initial current density of 0.24 mA/cm² on the passivated top surface and the sidewalls ($i_0 = 3.1 \mu\text{A/cm}^2$; $\alpha_c = 0.9$), which was increased gradually due to depolarization by SPS. The current density on the top surface and the sidewalls reached 3.4 mA/cm² by the end of 47 sec ($i_0 = 46 \mu\text{A/cm}^2$; $\alpha_c = 0.9$).



References

1. P.C. Andricacos, C. Uzoh, J. O. Dukovic, J. Horkans and H. Deligianni, *IBM J. of Res. and Dev.* 42(5), pp. 567-574, September, 1998
2. D. C. Edelstein, in Advanced Metallization Conference Proceedings in 1998, pp. 669-671, Mat. Res. Soc. 1999.
3. CELL-DESIGN[®], Computer Aided Design and Simulation of Electrochemical Cells, L-Chem, Inc. 13909 Larchmere Blvd. Shaker Heights, OH 44120.
4. Eugene Malyshev, Uziel Landau, and Sergey Chivilikhin, "Modeling the Deposit Thickness Distribution in Copper Electroplating of Semiconductor Wafer Interconnects", Paper # 190 c, Session TK (this Symposium); Proceedings of the AIChE Annual Meeting, San-Francisco, CA Nov. 2003
5. Uziel Landau, Proceedings of the D. N. Bennion Mem. Symp., R. E. White and J. Newman, Eds., The Electrochemical Society Proceedings Volume 94-9, 1994.
6. Uziel Landau, "Copper metallization of semiconductor interconnects – Issues and Prospects" Proceedings of the Electrochemical Soc., PV 2000-26, pp. 231-253. R. Opila et. al., Eds. (2000).
7. U. Landau, R. Akolkar, M. Bubnick and J. D'Urso, "Synergistic and Transient Effects of Additives in Copper Interconnect Metallization", Extended Abstract No. 612, 203rd Electrochemical Society Meeting, Paris, France, April 28-May 2 (2003).
8. Rohan Akolkar and Uziel Landau, "Additives Interactions During Copper Interconnect Metallization", Paper # 189 c, (this symposium); Proceedings of the AIChE Annual Meeting, , San-Francisco, CA Nov. 2003.
9. Rohan Akolkar and Uziel Landau, to be published.
10. P.C. Andricacos, C. Uzoh, J. O. Dukovic, J. Horkans and H. Deligianni, "Damascene copper electroplating for chip interconnects," *IBM J. of Res. and Dev.* 42(5), pp. 567-574, September (1998).
11. H. Deligianni, J. Horkans, K. Kwietniak, J. O. Dukovic, P. C. Andricacos, S. Boettcher, S. C. Seo, P. Locke, A. Simon, S. Seymour and S. Malhotra, "A Model of Superfill in Damascene Electroplating: Comparison of Feature Filling with Model Predictions," *The Electrochem. Soc. Meeting Abstracts*, Vol No. 2000-1, Abstract No. 368, The Electrochemical Society Meeting, Toronto, May (2000).
12. Y. Cao, P. Taephaisitphongse, R. Chalupa and A. C. West, "Three-Additive Model of Superfilling of Copper", *J. Electrochem. Soc.*, 148 (7), C466 (2001).
13. D. Josell, B. Baker, C. Witt, D. Wheeler and T. P. Moffat, *J. Electrochem. Soc.*, 149 (12), C637 (2002). D. Edelstein et al., Tech. Dig. IEEE Int. Elec. Dev. Mtg., Wash. D.C., Dec. 7-10, 1997, pp773-6.
14. M. Georgiadou, D. Veyret, R.L. Sani and R.C Alkire, "Simulation of Shape Evolution during Electrodeposition of Copper in the Presence of Additive," *J. Electrochem. Soc.* 148(1), pp C54-C58 (2001).
15. D. Veyeret and M. Georgiadou, 'Simulation of Pulse Plating in High-Aspect Ratio Trenches', Extended Abstract No. 767, Volume 2001-2, Meeting Abstracts, The 200th meeting of The Electrochemical Society, San-Francisco, CA, Sept. 2-7, 2001.